

PREPARED FOR SUBMISSION TO JCAP

Can massive primordial black holes be produced in mild waterfall hybrid inflation?

Masahiro Kawasaki^{a,b} and Yuichiro Tada^{a,b}

^aInstitute for Cosmic Ray Research, The University of Tokyo, Kashiwa, Chiba 277-8582, Japan

^bKavli Institute for the Physics and Mathematics of the Universe (WPI), UTIAS, The University of Tokyo, Kashiwa, Chiba 277-8583, Japan

E-mail: kawasaki@icrr.u-tokyo.ac.jp, yuichiro.tada@ipmu.jp

Abstract. We studied the possibility whether the massive primordial black holes (PBHs) surviving today can be produced in hybrid inflation. Though it is of great interest since such PBHs can be the candidate for dark matter or seeds of the supermassive black holes in galaxies, there have not been quantitatively complete works yet because of the non-perturbative behavior around the critical point of hybrid inflation. Therefore, combining the stochastic and δN formalism, we numerically calculated the curvature perturbations in a non-perturbative way and found, without any specific assumption of the types of hybrid inflation, PBHs are rather overproduced when the waterfall phase of hybrid inflation continues so long that the PBH scale is well enlarged and the corresponding PBH mass becomes sizable enough.

Keywords: inflation, primordial black holes

Contents

1	Introduction	1
2	Aspects of hybrid inflation	2
3	Parameter search	5
3.1	Stochastic formalism	5
3.2	Mean and variance of e-folds	7
3.3	PBH abundance	9
4	Exact power spectrum	11
5	Conclusions	13

1 Introduction

The primordial black holes (PBHs) are theoretically suggested black holes produced in the early universe. They are formed by the gravitational collapse of the Hubble patches which are $\mathcal{O}(1)$ denser than their surroundings in the radiation dominant [1–3]. The PBH abundance is connected to the properties of the primordial curvature perturbations, which determines how rare such quite overdense patches are. As an interesting point of the PBH, it is one of the well-studied candidates for dark matter (DM). While all windows for PBHs to be a main component of DMs seem to be closed recently [4], there may be some loopholes. For example, the constraints for around $10^{23-24} \text{ g} \sim 10^{-10} M_{\odot}$ from neutron stars are still under discussion (see e.g. [5–8] as related works).

Another important motivation of PBHs is to explain the seeds of supermassive black holes (SMBHs). Most galaxies including our Milky Way are thought to possess one or a few SMBHs whose masses reach to $10^{6-9.5} M_{\odot}$ in their centers [9], and moreover, such massive black holes have been found even at high redshifts as $z \sim 6-7$ [10, 11]. While the astrophysical production mechanism of (especially high- z) SMBHs has still been unknown, the literature suggested massive PBHs ($\sim 10^5 M_{\odot}$) can be the seeds of SMBHs [12]. Therefore, whether sufficiently massive PBHs can be produced (*naturally* if possible) or not is an important subject.

While various mechanisms to produce massive PBHs have been proposed (*double inflation*: [13–16], *running mass*: [17, 18], *curvaton*: [19]), we will focus on hybrid inflation in this paper. Hybrid inflation, which was originally proposed by Linde [20], is a combined model of chaotic and hilltop inflation. In this model, the inflationary universe is driven by the false vacuum energy of the so-called waterfall field, represented as ψ here, which is stabilized by the coupling to the other scalar inflaton, denoted by ϕ , at first. Then, when the inflaton’s vev becomes small due to the potential of itself and the coupling between ϕ and ψ gets to unable to stabilize the waterfall field, inflation will terminate by the second order phase transition of ψ . Hybrid inflation is an attractive model in the point that the initial condition problem is improved well in this model though it is small field inflation (namely the scalar fields’ vev does not exceed the Planck scale).

The mainstream of hybrid inflation is models where the inflaton’s slow-roll phase (called *valley phase* generically) continues more than 60 e-folds and the waterfall transition ends instantaneously. Among this type, the original model where the inflaton’s potential is given by simple mass term predicts blue-tilted curvature perturbations which have been excluded now, but the supersymmetric flat inflaton whose potential can be raised up logarithmically due to the Coleman-Weinberg correction can give a red-tilted spectrum [21], and moreover, it has been suggested that the additional linear potential from the soft supersymmetry (SUSY) breaking can realize $n_s \sim 0.96$ [22], which is in the Planck’s sweet spot [23]. Another direction of realizations of hybrid inflation is the long-waterfall models [24–28]. In these models, ψ ’s potential is so flat that the waterfall phase continues more than 60 e-folds like hilltop inflation.

In this paper, we will concentrate on the intermediate case, namely the mild-waterfall models where the waterfall phase continues more than a few e-folds but less than 60 e-folds. An attractive point of the mild case is that very massive PBHs can be produced a lot. That is because the perturbations can grow much around the phase transition critical point due to the flatness of the (especially ψ ’s) potential and such perturbations will be inflated during the long-lasting waterfall phase. Though the massive PBH production in mild-waterfall hybrid inflation has been discussed for a long time [29–32], there is still not a quantitatively complete work because of its non-perturbative difficulty. Around the critical point, the field perturbations affect the background dynamics itself, therefore intrinsically the scalar fields cannot be treated perturbatively during the phase transition (see [33] for example).

Recently, in refs. [34, 35],¹ we have proposed some non-perturbative algorithm to calculate the power spectrum of curvature perturbations in the stochastic formalism [37–43]. Especially in ref. [35], the power spectrum in mild-waterfall hybrid inflation was calculated without perturbative expansions with respect to ϕ and ψ . Following these works, we perform a wide parameter search in this paper with use of our algorithm and conclude that PBHs are rather overproduced in most of the mild-waterfall cases. Also we clarify the parameter constraints from the PBH constraints.

The rest of the paper is organized as follows. In section 2, we introduce hybrid inflation and briefly review the analytic approximations for the scalar dynamics and curvature perturbations, following ref. [32]. In section 3, we perform a rough parameter search and find that PBHs are overproduced in the mild-waterfall cases. Also concrete constraints for parameters are obtained as a main result of the paper. In section 4, we show the exact power spectra of the curvature perturbations as a consistency check of the previous parameter search with use of our algorithm. Finally section 5 is devoted to conclusions.

2 Aspects of hybrid inflation

In this section, we would like to introduce hybrid inflation and its various aspects. Throughout this paper, we do not assume any specific UV-theoretical motivation like SUSY and simply refer the models whose potential is given by the following form as *hybrid inflation*.

$$V(\phi, \psi) = V(\phi) + \Lambda^4 \left[\left(1 - \frac{\psi^2}{M^2} \right)^2 + 2 \frac{\phi^2 \psi^2}{\phi_c^2 M^2} \right]. \quad (2.1)$$

Here ϕ and ψ are two scalar field which are called *inflaton* and *waterfall* fields respectively, while Λ , M , and ϕ_c are dimensionful model parameters. As the second term indicates, the

¹Recently Vennin and Starobinsky has verified this formalism and found some analytic expressions with use of techniques of stochastic calculus [36].

sign of the ψ 's effective mass squared, $m_{\psi,\text{eff}}^2|_{\psi\sim 0} = \partial_\psi^2 V|_{\psi\sim 0} = 2\frac{\Lambda^4}{M^2}\left(\frac{\phi^2}{\phi_c^2} - 1\right)$, is determined by ϕ 's vev. Namely, if ϕ 's vev is larger than the critical value ϕ_c , ψ is stabilized to the origin due to its positive mass squared. Then, with the pseudo-flat $V(\phi)$ which is minimized around the origin, the inflaton can undergoes a slow-roll to its minimum and *switch on* the tachyonic property of the waterfall field when ϕ reaches ϕ_c . Subsequently inflation will be ended by the second order phase transition of ψ .

The stage before ϕ reaches ϕ_c is called *valley phase* and that after ϕ_c is referred as *waterfall phase* generically. Though the waterfall phase basically ends instantaneously due to the tachyonic instability, the literatures [24–28] suggested the possibility of the long-lasting waterfall. In this paper, we concentrate on the mild-waterfall case where the waterfall phase continues more than a few e-folds but less than about 60 e-folds. That is, the phase transition occurs around the middle between the horizon exit of the scale of the cosmic microwave background (CMB) and the end of inflation. In such cases, ϕ 's vev is almost equal to ϕ_c during about 60 e-folds and therefore we can Taylor expand the inflaton's potential $V(\phi)$ around ϕ_c regardless of the motivating UV theories. Namely, adopting the notation of ref. [32], we analyze the following form of the potential.

$$V(\phi, \psi) = \Lambda^4 \left[\left(1 - \frac{\psi^2}{M^2}\right)^2 + 2\frac{\phi^2\psi^2}{\phi_c^2 M^2} + \frac{\phi - \phi_c}{\mu_1} - \frac{(\phi - \phi_c)^2}{\mu_2^2} \right]. \quad (2.2)$$

It has five dimensionful parameters as Λ , M , ϕ_c , μ_1 , and μ_2 . Among them, two d.o.f. can be fixed by the information of the amplitude and tilt of the power spectrum of the curvature perturbations on the CMB scale. In the mild-waterfall case, the CMB scale corresponds with the point in the valley phase, where the waterfall field is still irrelevant due to its large mass. Therefore the perturbations can be analyzed linearly as the simple single-field slow-roll case. At first the slow-roll parameters are given by,

$$\epsilon_V = \frac{M_p^2}{2} \left(\frac{V_\phi}{V} \right) \bigg|_{\phi\sim\phi_c, \psi\sim 0} \simeq \frac{M_p^2}{2\mu_1^2}, \quad \eta_V = M_p^2 \frac{V_{\phi\phi}}{V} \bigg|_{\phi\sim\phi_c, \psi\sim 0} \simeq -\frac{2M_p^2}{\mu_2^2}, \quad (2.3)$$

where M_p is the reduced Planck mass $\sqrt{8\pi G}^{-1} \simeq 2.4 \times 10^{18} \text{ GeV} \simeq 4.3 \times 10^{-6} \text{ g}$. The spectral index n_s is, in the slow-roll limit,

$$n_s = 1 - 6\epsilon_V + 2\eta_V \simeq 1 - \frac{4M_p^2}{\mu_2^2}, \quad (2.4)$$

where we assumed that η_V dominates ϵ_V (as can be checked easily for specific parameter regions shown in the following sections), which is the case for small field inflation. From this relation, with the Planck's best fit value $n_s \simeq 0.9655$ [23], μ_2 should be fixed to,

$$\frac{\mu_2}{M_p} = \frac{2}{\sqrt{1 - n_s}} \simeq 11. \quad (2.5)$$

Also the amplitude of the power spectrum is given by,

$$A_s = \frac{1}{24\pi^2 M_p^4} \frac{V}{\epsilon_V} \simeq \frac{\Lambda^4 \mu_1^2}{12\pi^2 M_p^6}. \quad (2.6)$$

Again it should be fixed by the Planck's result $A_s \simeq 2.198 \times 10^{-9}$, which gives the following relation.

$$\left(\frac{\Lambda}{M_p}\right)^4 \simeq 2.198 \times 10^{-9} \times 12\pi^2 \left(\frac{\mu_1}{M_p}\right)^{-2}. \quad (2.7)$$

In the following sections, we will fix Λ with this constraint and take M, ϕ_c and μ_1 as free parameters.

In ref. [32], Clesse and Garcia-Bellido (CG) analytically approximated the curvature perturbations during the waterfall phase and estimated the PBH abundance. At first they calculated the variance of the waterfall field at the critical point, namely $\sigma_\psi^2 = \langle \psi^2 \rangle|_{\phi=\phi_c}$, in the stochastic formalism which we will describe in the next section, as,

$$\sigma_\psi = \left(\frac{\sqrt{2}\Lambda^4 M \phi_c^{1/2} \mu_1^{1/2}}{96\pi^{3/2} M_p^4} \right)^{1/2}. \quad (2.8)$$

Then it was used as an initial condition of ψ at the beginning of the waterfall phase, that is $\psi_0 = \psi|_{\phi=\phi_c} \simeq \sigma_\psi$. The curvature perturbations were finally calculated by the standard linear perturbation theory. We briefly review the results below, while the details are omitted.

With the potential (2.2), the slow-roll e.o.m. is given by,

$$\begin{cases} 3H\dot{\phi} = -V_\phi \simeq -\frac{\Lambda^4}{\mu_1} - \frac{4\Lambda^4\psi^2}{M^2\phi_c^2}\phi, \\ 3H\dot{\psi} = -V_\psi \simeq -\frac{4\Lambda^4}{M^2} \left(\frac{\phi^2}{\phi_c^2} - 1 \right) \psi, \end{cases} \quad (2.9)$$

$$\quad (2.10)$$

where V_ϕ and V_ψ denotes the derivatives of the potential with respect to ϕ and ψ . Here we omitted the higher-order terms. Then CG divided the waterfall phase into two stage; in the first phase-1 the second term of the right side of eq. (2.9) is negligible and in the phase-2 that dominates the first term. With the approximation $H^2 \simeq \Lambda^4/3M_p^2$, the e-folds for the phase-1 and 2 can be calculated as,

$$N_1 \simeq \frac{\sqrt{\chi_2} M \phi_c^{1/2} \mu_1^{1/2}}{2M_p^2}, \quad N_2 \simeq \frac{M \phi_c^{1/2} \mu_1^{1/2}}{4M_p^2 \sqrt{\chi_2}}, \quad (2.11)$$

where,

$$\chi_2 = \log \left(\frac{\phi_c^{1/2} M}{2\mu_1^{1/2} \psi_0} \right), \quad (2.12)$$

gives the ψ 's field value at the transition point between phase-1 and 2 by $\psi = \psi_0 e^{\chi_2}$. Therefore the total e-folds for the waterfall phase is given by,

$$N_{\text{water}} \simeq N_1 + N_2 \simeq \left(\frac{\sqrt{\chi_2}}{2} + \frac{1}{4\sqrt{\chi_2}} \right) \frac{M \phi_c^{1/2} \mu_1^{1/2}}{M_p^2}. \quad (2.13)$$

Also, according to the δN formalism [44–48], the power spectrum of the curvature perturbations can, in the linear perturbation theory, be approximated by,

$$\mathcal{P}_\zeta(k) = \frac{k^3}{2\pi^2} \int d^3x \langle \zeta(0)\zeta(\mathbf{x}) \rangle e^{-i\mathbf{k}\cdot\mathbf{x}} \simeq \frac{H^2}{(2\pi)^2} (N_\phi^2 + N_\psi^2) \Big|_{aH=k}, \quad (2.14)$$

where N_ϕ and N_ψ are the derivatives of the backward e-folds with respect to ϕ and ψ respectively. Assuming the dominant contribution comes from the variation of the phase-1 e-folds N_1 due to the ψ 's fluctuations, the power spectrum is given by,

$$\mathcal{P}_\zeta(k) \simeq \frac{\Lambda^4 M^2 \phi_c \mu_1}{192 \pi^2 M_p^6 \chi_2 \psi_k^2}, \quad (2.15)$$

with $\psi_k = \psi_0 e^{\chi_k}$, $\chi_k = 4\phi_c \mu_1 \xi_k^2 / M^2$, and $\xi_k = -M_p^2(N_1 + N_2 - N_k) / (\phi_c \mu_1)$. N_k is the backward e-folds corresponding with considered comoving scale k , namely $k = e^{-N_k} k_f$ where k_f is the comoving horizon scale aH at the end of inflation. The power spectrum is maximal at the critical point as,

$$\mathcal{P}_{\zeta, \max} \simeq \frac{\Lambda^4 M^2 \phi_c \mu_1}{192 \pi^2 M_p^6 \chi_2 \psi_0^2} = \frac{M \phi_c^{1/2} \mu_1^{1/2}}{2 \sqrt{2\pi} M_p^2 \chi_2}. \quad (2.16)$$

There are two key points in these results. The first one is that both of the e-folding numbers for the waterfall phase N_{water} and the maximum of the power spectrum $\mathcal{P}_{\zeta, \max}$ depend almost only on the specific parameter combination $M^2 \phi_c \mu_1 / M_p^4$ called Π^2 by CG, except for the small logarithmic dependence due to χ_2 . This property will be checked in the next section with use of the stochastic formalism, and it will be confirmed that the parameter Π^2 indeed plays the key role beyond the linear approximation. As the second and more important point, the power spectrum given by CG has its maximum at the critical point. This will be disproved in section 4 by showing that the exact power spectra have peaks *well after* the critical point. That is because the dynamics of ψ is still dominated by the stochastic noise around ϕ_c and its fluctuations here do not affect the average trajectories well after the critical point so much. Namely, the adiabatic perturbations around ϕ_c are still given almost only by ϕ , and hence small. After that, the ψ 's fluctuations also start to contribute to the adiabatic mode and the curvature perturbations get grown.

3 Parameter search

Though we reviewed the result in the linear perturbation theory in the previous section, the dynamics of the waterfall field around the critical point is actually dominated by the Hubble fluctuations. Therefore the linear perturbation with respect to ψ around the critical point essentially breaks down (c.f. [33]). Accordingly we calculate the curvature perturbations without the perturbative expansions with respect to ϕ and ψ with use of the stochastic formalism. In this section we introduce the stochastic formalism at first. Then we calculate the curvature perturbations in the wide parameter region. From their results, we conclude that PBHs are overproduced in the mild-waterfall cases as a main claim of this paper.

3.1 Stochastic formalism

The stochastic formalism was proposed by Starobinsky in 1986 [37] (see also [38–43]). In this formalism, the superhorizon coarse-grained fields, namely,

$$\phi_{\text{IR}}(t, \mathbf{x}) = \int \frac{d^3 k}{(2\pi)^3} W\left(\frac{k}{\epsilon a H}\right) e^{i\mathbf{k} \cdot \mathbf{x}} \phi_{\mathbf{k}}(t), \quad (3.1)$$

are treated as the classical background fields. Here $W(k/k_s)$ is a window function and ϵ is a small positive parameter. As a window function, the simple step function $\theta(\epsilon a H - k)$ is

often used for brevity. ϵ divides the scalar fields into the classicalized part and the quantum part. That is, the modes for $k < \epsilon aH$ are well classicalized and can be treated as classical fields, while the modes for $k > \epsilon aH$ should be assumed to be the quantum operators. To take sufficiently superhorizon modes and also validate the perturbative expansions with respect to ϵ which we use below, ϵ should be less than unity. In this paper the value of 0.01 is used for ϵ .

For the above coarse-grained fields, the e.o.m. reads [49],

$$\begin{cases} \frac{d\phi_{\text{IR},i}}{dN} = \frac{\pi_{\text{IR},i}}{H} + \mathcal{P}_{\phi_i}^{1/2}(k = \epsilon aH)\xi_i, \\ \frac{d\pi_{\text{IR},i}}{dN} = -3\pi_{\text{IR},i} - \frac{V_i}{H}, \end{cases} \quad (3.2)$$

in the leading order with respect to ϵ . $\mathcal{P}_{\phi_i}^{1/2}$ denotes the power spectrum of ϕ_i , i.e. $\mathcal{P}_{\phi_i}(k) = \frac{k^3}{2\pi^2} \int d^3x \langle \phi_i(0)\phi_i(\mathbf{x}) \rangle e^{-i\mathbf{k}\cdot\mathbf{x}}$. The subscript i labels the flavors of the scalar fields for the multi-field cases. Without the term of ξ_i , it is recovered to the standard e.o.m. for the homogenous fields. This ξ term as an important difference is interpreted as a classical Gaussian random variable having following stochastic properties.²

$$\begin{cases} \langle \xi_i(N, \mathbf{x}) \rangle = 0, \\ \langle \xi_i(N, \mathbf{x})\xi_j(N', \mathbf{x}') \rangle = \delta_{ij} \frac{\sin(\epsilon aHr)}{\epsilon aHr} \delta(N - N'), \quad r = |\mathbf{x} - \mathbf{x}'|. \end{cases} \quad (3.3)$$

For the coarse-grained fields, $\frac{\sin(\epsilon aHr)}{\epsilon aHr}$ can be approximated by $\theta(1 - \epsilon aHr)$. The delta function type property for the time variable comes from the fact that we used the sharp window function for eq. (3.1). Anyway it represents the fact that *the superhorizon coarse-grained fields receive the Gaussian white noise independent for each Hubble patch and its amplitude is given by the scalar fields' perturbations $\mathcal{P}_{\phi_i}^{1/2}$* . This noise term comes from the inflow of the UV part $\phi_{\text{UV}} = \phi - \phi_{\text{IR}}$ into the IR part for every time. As we indicated, the UV part originally behaves as a quantum field but it is redshifted and classicalized at the time of $k = \epsilon aH$ to join in the IR part. At this time the exact field value of this joining mode cannot be determined due to its quantum property. Instead it is interpreted as a classical random variable and its amplitude can be calculated in quantum field theory as \mathcal{P}_{ϕ_i} of course.

Due to the noise term, every Hubble patch is assumed to evolve independently in the stochastic formalism. In this sense, the all background parameter values in eq. (3.2), namely H , V_i , and \mathcal{P}_{ϕ_i} , should be determined in each Hubble patch by the scalar field values of that patch. Inversely, if one concentrate on the dynamics of one Hubble patch, the e.o.m. reduces

²Here we assume there is no correlation between the different flavors of ξ . However the correlations between them due to the interactions before the horizon exit can be also included. In this paper, we omit them for simplicity after easily checked that they do not affect the result at all.

to the following self-closed Langevin equations.

$$\begin{cases} \frac{d\phi_i}{dN}(N) = \frac{\pi_i}{H}(N) + \mathcal{P}_{\phi_i}^{1/2}(N)\xi_i(N), \\ \frac{d\pi_i}{dN}(N) = -3\pi_i(N) - \frac{V_i}{H}(N), \\ V_i(N) = V_i(\phi_1(N), \phi_2(N), \dots), \\ 3M_p^2 H^2(N) = \sum_i \frac{\pi_i^2}{2} + V(\phi_1(N), \phi_2(N), \dots), \\ \langle \xi_i(N) \rangle = 0, \\ \langle \xi_i(N)\xi_j(N') \rangle = \delta_{ij}\delta(N - N'). \end{cases} \quad (3.4)$$

However in regards to \mathcal{P}_{ϕ_i} , one should calculate the dynamics of all subhorizon modes with the above Langevin eq. to obtain the value of them, strictly speaking. In this paper we approximate them by,

$$\mathcal{P}_{\phi_i}^{1/2} \simeq \frac{H}{2\pi} \left(\frac{k}{2aH} \right)^{\frac{m_i^2}{3H^2}} = \frac{H}{2\pi} \left(\frac{\epsilon}{2} \right)^{\frac{V_{ii}}{3H^2}}, \quad (3.5)$$

for simplicity. In the following sections, we numerically solve these equations (3.4) and (3.5).

3.2 Mean and variance of e-folds

As we saw in the previous section, the stochastic formalism gives the e.o.m. for the scalar fields coarse-grained on the horizon scale. Therefore the dynamics of one spatial point in the stochastic formalism can be regarded as that of one Hubble patch. Namely, in the stochastic formalism, the scalar field in each Hubble patch behaves as a Brownian motion drifted by the potential force. On the other hand, according to the δN formalism [44–48], the gauge invariant curvature perturbations on the superhorizon scale are given by the difference of the e-folds between the initial flat slice and the final uniform density slice. That is, since the dynamics of each Hubble patch automatically fluctuates due to the noise, the e-folding numbers also vary over the universe and their fluctuations are nothing but the curvature perturbations. Strictly speaking, the obtained curvature perturbations are coarse-grained values on the horizon scale at the end of inflation.

Let us describe the method more concretely. At first, one must determine the initial flat slice in the valley phase and the final uniform density slice around the end of inflation. Here, regarding the initial flat slice, note that in the valley phase inflation can be approximated as the single-field case and moreover the curvature perturbations are much smaller than those expected in the waterfall phase. Therefore, neglecting the curvature perturbations, the initial flat slice can be approximated by the uniform ϕ slice and the ψ 's field value is almost irrelevant. Next, making many realizations of the Langevin equations from the initial field values to the final energy density value, one can obtain various realizations of the e-folding numbers. Their deviations from the mean value $\langle N \rangle$ are nothing but the data set of the coarse-grained curvature perturbations. Though the information of the correlation function like $\langle \zeta(\mathbf{x}_1)\zeta(\mathbf{x}_2) \rangle$ for $\mathbf{x}_1 \neq \mathbf{x}_2$ cannot be derived at this time, at least the probability distribution function (PDF) of the coarse-grained curvature perturbations can be obtained up to the realization errors. With use of this PDF, one can calculate the formation rate of PBHs whose masses are larger than that corresponding with the horizon scale at the end of

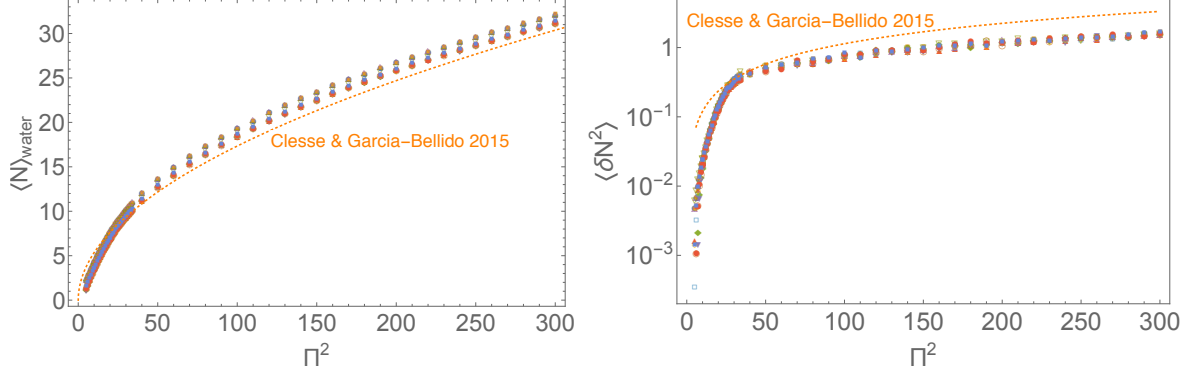


Figure 1. The mean e-folds of the waterfall phase (left panel) and the variance of their perturbations (right panel) vs. $\Pi^2 = M^2 \phi_c \mu_1 / M_p^4$ for various parameter sets in the searching region (3.6). μ_1 is varied for each set of M and ϕ_c . There are 12 sets of (M, ϕ_c) represented by different markers although they cannot distinguished in the figure. 2000 realizations are made for each data point. It is clearly shown that both of $\langle N \rangle$ and $\langle \delta N^2 \rangle$ depend almost only on Π^2 as ref. [32] suggested. However, while their results which are represented by orange dotted lines are well consistent with our calculations for $\langle N \rangle$, there are factor differences in $\langle \delta N^2 \rangle$. Anyway these plots indicate Π^2 should be less than about 10 to satisfy the PBH constraint $\langle \delta N^2 \rangle \lesssim 0.01$ and it means the waterfall phase cannot continue more than about 5 e-folds.

inflation. In this section, let us roughly estimate the PBH abundance by this quantity and find the parameter constraints. In the next section, we will calculate the exact power spectra and this procedure will be validated.

For parameter search, we used the following three searching regions.

- $10^{-4} M_p \leq M \leq 10^{-1} M_p$, $\phi_c = \sqrt{2} M$, (SUSY like assumption)
 - $M = 0.1 M_p$, $10^{-4} M_p \leq \phi_c \leq 10^{-1} M_p$,
 - $10^{-4} M_p \leq M \leq 10^{-1} M_p$, $\phi_c = 0.1 M_p$.
- (3.6)

μ_1 is also varied so that $\Pi^2 = M^2 \phi_c \mu_1 / M_p^4$ takes the value up to 300. Λ is given by eq. (2.7) for each value of μ_1 . In figure 1, we plot the mean e-folds for the waterfall phase $\langle N \rangle_{\text{water}}$ and the variance of their perturbations $\langle \delta N^2 \rangle = \langle N^2 \rangle - \langle N \rangle^2$ vs. $\Pi^2 = M^2 \phi_c \mu_1 / M_p^4$ for various parameters in the above searching region. μ_1 is varied for each parameter set (M, ϕ_c) . Also the CG's analytic results (2.13) and (2.15) are shown as orange dotted lines. Here note that the variance and the power spectrum are related by,

$$\langle \delta N^2 \rangle \simeq \int_0^{\langle N \rangle_{\text{water}}} \mathcal{P}_\zeta(k) dN_s. \quad (3.7)$$

From this figure, it is found that the mean e-folds $\langle N \rangle$ obtained in the stochastic formalism is well fitted by the CG's result. On the other hand, there are factor differences in the variance $\langle \delta N^2 \rangle$. It clearly shows the non-perturbative effects which CG did not include. However at least it can be said that the full result of $\langle \delta N^2 \rangle$ also depends only on the specific parameter combination $\Pi^2 = M^2 \phi_c \mu_1 / M_p^4$. Having in mind that the variance of the curvature perturbations should be roughly less than 10^{-2} at most not to overproduce PBHs as we will show in the next subsection, it can be seen that Π^2 should be less than around 10, which indicates the waterfall phase cannot continue more than about 5 e-folds.

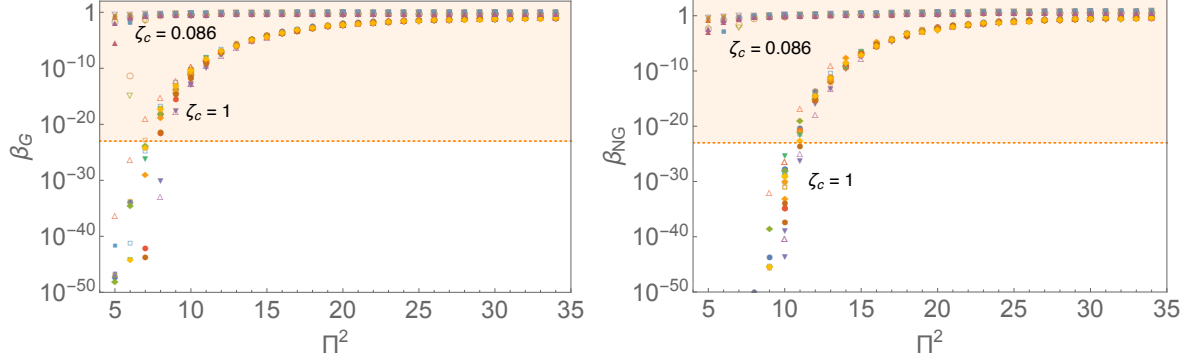


Figure 2. Left panel: the plot of the PBH abundance in the Gaussian assumption β_G (3.10) with use of the variance shown in figure 1. Namely this is for very light PBHs as $M_{\text{PBH}} \sim M_p^2/H_{\text{inf}}$, contracting that we want massive PBHs. It will be validate in the next section. The bottom group is for $\zeta_c = 1$ while the upper group is for $\zeta_c \simeq 0.086$ [52]. Also the orange dotted line represents the typical constraints for light PBHs ($\lesssim 10^{15}$ g), namely $\beta \lesssim 10^{-23}$. If $\zeta_c \simeq 0.086$, there is no appropriate value of Π^2 with which PBHs are not overproduced. On the other hand, if $\zeta_c = 1$, the PBH constraints indicate $\Pi^2 \lesssim 8$, which means the waterfall phase can continue few e-folds as shown in figure 1. Right panel: the same plot with NG corrections (3.12). Though the results for $\zeta_c \simeq 0.086$ are hardly different, the PBH abundance for $\zeta_c = 1$ is suppressed for low Π^2 compared to the value without NG corrections. Then the constraints are slightly weakened to $\Pi^2 \lesssim 11$ but the duration of the waterfall phase is still as short as 4–5 e-folds.

3.3 PBH abundance

In this subsection, we estimate the PBH abundance including the non-Gaussian (NG) effects. Following the Press-Schechter approach [50], if the coarse-grained curvature perturbations ζ_s have the PDF $P(\zeta_s)$, the formation rate of PBHs which are more massive than the mass corresponding with the coarse-graining scale is given by,

$$\beta(> M_{\text{PBH}}) = 2 \int_{\zeta_c}^{\infty} P(\zeta_s) d\zeta_s, \quad (3.8)$$

where ζ_c is the threshold for the PBH formation. The factor 2 is conventional to include the effects of merges and accretions. For the case of PBHs, the mass M_{PBH} is related to the coarse-graining comoving scale R_s by,

$$M_{\text{PBH}} \simeq \frac{M_p^2}{H_{\text{inf}}} (k_f R_s)^2 \simeq \frac{M_p^2}{H_{\text{inf}}} e^{2N_s} = 1.0 \times 10^4 \text{ g} \left(\frac{H_{\text{inf}}}{10^9 \text{ GeV}} \right)^{-1} e^{2N_s}. \quad (3.9)$$

Here H_{inf} is the Hubble parameter at the end of inflation and N_s denotes the corresponding backward e-folds, $R_s^{-1} = k_f e^{-N_s}$. We assumed that reheating occurs soon after inflation. If the power spectrum has a sharp peak, which will be validated in the next section, PBHs are formed almost only on the peak scale and the above β with the coarse-graining scale being the peak scale can be directly used to be constrained.

If one assumes the curvature perturbations follow the Gaussian distribution, β can be easily estimated by,³

$$\beta_G = 2 \int_{\zeta_c}^{\infty} \frac{1}{\sqrt{2\pi\sigma_s^2}} e^{-\zeta_s^2/2\sigma_s^2} d\zeta_s, \quad (3.10)$$

³Though we used the variance of the coarse-grained curvature perturbations here, the authors of [51] claimed that the power spectrum on the considered scale should be used instead of the variance. That is

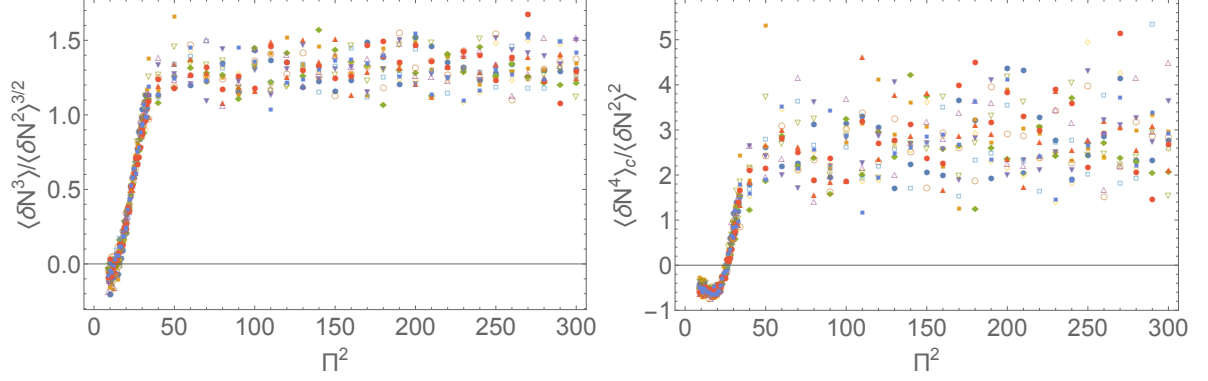


Figure 3. The skewness $S^{(3)} = \langle \delta N^3 \rangle / \langle \delta N^2 \rangle^{3/2}$ and kurtosis $S^{(4)} = \langle \delta N^4 \rangle_c / \langle \delta N^2 \rangle^2$ where $\langle \delta N^4 \rangle_c = \langle \delta N^4 \rangle - 3 \langle \delta N^2 \rangle^2$ is a connected part of the forth moment. It clearly indicates the non-negligible $\mathcal{O}(1)$ NG.

where σ_s^2 denotes the variance of the coarse-grained curvature perturbations, namely, with use of some window function $W(kR_s)$,

$$\sigma_s^2 = \langle \zeta_s^2 \rangle = \int W^2(kR_s) \mathcal{P}_\zeta(k) d \log k. \quad (3.11)$$

On the left panel of figure 2, we plot the β_G with use of $\langle \delta N^2 \rangle$ shown in figure 1 as σ_s^2 for different two threshold values, that is, the simple assumption $\zeta_c = 1$ and the recent analytic prediction by Harada et al [52], $\zeta_c = \frac{1}{3} \log \frac{3(\chi_a - \sin \chi_a \cos \chi_a)}{2 \sin^3 \chi_a} \Big|_{\chi_a = \pi \sqrt{\omega}/(1+3\omega)} \simeq 0.086$ where ω is the e.o.s. for radiation, $p/\rho = 1/3$. Also we show the typical constraints for light PBHs $\beta_G \sim 10^{-23}$ as an indicator [53].⁴ Incidentally this value corresponds with 10 sigma rarity, i.e. $\zeta_c \sim 10\sigma_s$. Therefore this constraint roughly indicates $\mathcal{P}_\zeta \sim \sigma_s^2 \lesssim 0.01$ for $\zeta_c = 1$ as mentioned previously. The figure shows Π^2 should be less than around 8 for the case $\zeta_c = 1$, which means the waterfall phase can continue few e-folds. Also there is almost no proper parameter set with which PBHs are not overproduced if $\zeta_c \simeq 0.086$. Here we used the variance obtained in the previous subsection, and please recall that it means coarse-graining scale is the Hubble scale at the end of inflation, that is, the corresponding PBH mass is quite small as $M_{\text{PBH}} \simeq M_p^2/H_{\text{inf}}$. Indeed it will be validate in the next section as we will show that the power spectrum for the case $\Pi^2 \lesssim \mathcal{O}(10)$ has a peak almost around the end of inflation.

On the other hand, the curvature perturbations produced around the critical point are naively thought to have NG as indicated by its non-perturbativity. In figure 3, we show the skewness $S^{(3)} = \langle \delta N^3 \rangle / \langle \delta N^2 \rangle^{3/2}$ and kurtosis $S^{(4)} = \langle \delta N^4 \rangle_c / \langle \delta N^2 \rangle^2$ where $\langle \delta N^4 \rangle_c = \langle \delta N^4 \rangle - 3 \langle \delta N^2 \rangle^2$ is a connected part of the forth moment. These values van-

because the curvature perturbations are undamped quantities even on superhorizon scales and therefore the variance includes the much superhorizon modes, which should not affect the PBH formation. However now the power spectrum has a sharp peak as we will show in the next section, and the larger scale modes than the peak scale are already suppressed. Therefore using the variance will not overestimate the PBH abundance so much. Since we would like to include the NG effects by the form of the third and forth moment, namely $\langle \delta N_s^3 \rangle$ and $\langle \delta N_s^4 \rangle$, we used the variance $\langle \delta N_s^2 \rangle$ instead of the power spectrum.

⁴Though we want massive PBHs $\gtrsim 10^{15} \text{ g}$, we will find such massive ones cannot be produced with proper abundance in hybrid inflation and then we used the constraints for light PBHs $\lesssim 10^{15} \text{ g}$.

ish in a pure Gaussian case, so non-zero values of them directly indicate the NG of the curvature perturbations. As we predicted, these plots show non-negligible $\mathcal{O}(1)$ NG.⁵

These NG modifies the PDF of the curvature perturbations and then β is given by,

$$\begin{aligned}\beta_{\text{NG}} &\simeq \frac{2}{\sqrt{2\pi}} \int_{\nu}^{\infty} d\alpha \exp \left[\sum_{n=3}^4 \frac{(-1)^n}{n!} S^{(n)} \frac{\partial^n}{\partial \alpha^n} \right] \exp \left[-\frac{\alpha^2}{2} \right] \\ &\simeq \sqrt{\frac{2}{\pi}} \frac{1}{\nu} \exp \left[\sum_{n=3}^4 \frac{\nu^2}{n!} S^{(n)} \right] e^{-\nu^2/2},\end{aligned}\tag{3.12}$$

where ν is defined by $\nu = \zeta_c/\sigma_s$ and we used the high peak limit $\nu \gg 1$ in the second line. Though we truncated them here, it is possible to include the higher order terms than forth order (see also appendix K of ref. [54]). This modified probability is plotted on the right panel in figure 2. Comparing to the Gaussian case (left panel), it can be seen that the probability for small Π^2 is suppressed for $\zeta_c = 1$, while the result for $\zeta_c = 0.086$ hardly changes. As a result, the constraint for Π^2 in the $\zeta_c = 1$ case is weakened to $\Pi^2 \lesssim 11$, which corresponds with $\langle N \rangle_{\text{water}} \lesssim 4$.

Let us briefly summarize the above results here. We calculated e-folds numerically in the stochastic formalism and checked that the mean e-folds for the waterfall phase and their variance depend almost only on some specific parameter combination $\Pi^2 = M^2 \phi_c \mu_1 / M_p^4$. However simultaneously it was found that the variance of the perturbations becomes large for mild-waterfall hybrid inflation. In fact, if $\zeta_c = 0.086$ [52], there is no parameter region where PBHs are not overproduced. Only if the PBH mass given by eq. (3.9) is lighter than 10^9 g, the constraint can be avoided because such PBHs are evaporated before big-bang nucleosynthesis (BBN). On the other hand, if the threshold is as high as $\zeta_c = 1$, the PBH overproduction roughly gives the parameter constraint as $\Pi^2 \lesssim 8$ (or 11 with NG corrections) which means the waterfall phase can continue few e-folds. It is too short to produce PBHs massive enough to be DMs or seeds of SMBHs. This is the main result of this paper.

4 Exact power spectrum

In the previous section, we calculated the PBH abundance with use of the curvature perturbations coarse-grained on the Hubble scale at the end of inflation. However, to obtain the main contribution to the PBH abundance, one must set the coarse-graining scale on the peak scale of the power spectrum. In this section, we show the power spectrum for small Π^2 ($\lesssim 50$) indeed has a peak almost around the end of inflation with use of our algorithm [34, 35].

Let us briefly review the algorithm at first. As mentioned repeatedly, in the stochastic formalism the dynamics in each Hubble patch is treated as an individual Brownian motion drifted by the potential force. The correlative information for two distant points is imprinted in when those two points are separated farther than the horizon scale. That is, while the scalar fields on two points evolves conjointly before the horizon exit, they start moving individually due to the non-correlating noise after their distance is larger than the Hubble size. It means the perturbations of the e-folding numbers obtained for the paths branching

⁵However the NG is not as large as has been considered. Refs. [30, 31] concluded the curvature perturbations have a negative chi-squared type distribution, namely $\zeta(\mathbf{x}) = -(g^2(\mathbf{x}) - \langle g^2 \rangle)$, where g is a Gaussian field. But this distribution type gives $S^{(3)} = -2\sqrt{2}$ and $S^{(4)} = 12$ which are larger enough than our result. Therefore our calculations give less NG curvature perturbations than the simple chi-squared ansatz.

from one field-phase-space point include only the modes which exit the horizon between the branching time and the end of inflation. Thus the following relation is satisfied.

$$\langle \delta N^2 \rangle = \int_{\log k_f - \langle N \rangle}^{\log k_f} \mathcal{P}_\zeta d \log k, \quad (4.1)$$

where $\langle N \rangle$ is the mean e-folding number from the branching point to the end of inflation. Inversely the power spectrum can be obtained from changing the branching point slightly as,

$$\mathcal{P}_\zeta(k) = \frac{d}{d \langle N \rangle} \langle \delta N^2 \rangle \Big|_{\langle N \rangle = \log(k_f/k)}. \quad (4.2)$$

While the branching point vev and the mean e-folds have a one-to-one correspondence in the single-field slow-roll case, there is only the uniform mean e-folds hypersurface on the field phase space in the multi-field case. Therefore the branching points should be properly weighted by the realization probability, which is reproduced by making various sample paths.

Concretely, we use the following algorithm.

1. Determine the initial field value from which the mean e-folds is about 60. It represents the field value of our observable universe at 60 e-folds before the end of inflation.⁶
2. Make one sample path by integrating the Langevin eqs. (3.4) and (3.5) from the initial field value. It shows the dynamics of some Hubble patch in our observable universe.
3. Produce various realizations branching from some point on the produced sample path and calculate the e-folds for them to the final uniform density surface around the end of inflation. They give the mean and variance of the e-folds, referred as $\langle N_1 \rangle$ and $\langle \delta N_1^2 \rangle$ here.
4. Repeat the procedure 3 with slightly different branching point to obtain another set of the mean and variance $\langle N_2 \rangle$ and $\langle \delta N_2^2 \rangle$. Then the power spectrum on the scale $k \simeq k_f e^{-((N_1) + \langle N_2 \rangle)/2}$ can be approximated by,

$$\mathcal{P}_\zeta(k) \simeq \frac{\langle \delta N_1^2 \rangle - \langle \delta N_2^2 \rangle}{\langle N_1 \rangle - \langle N_2 \rangle}. \quad (4.3)$$

This power spectrum is obtained from the paths branching from one sample path. Therefore this result is valid only in the region spatially near to that sample path.

5. To obtain the power spectrum valid over our universe, iterate the procedure 2–4 and average the obtained power spectra. This averaged one represents the true power spectrum obtained in our observable universe.

With use of the above algorithm, we calculate the power spectrum for $\Pi^2 = 10, 20, 30, 40$, and 50, and the results are shown in figure 4. Also the times when the paths pass the critical point are indicated by vertical gray dotted lines. The plot shows that it takes about 10 e-folds

⁶The power spectrum obtained by the following procedure depends on this initial field value in principle. This ambiguity is not only for our algorithm. The predictability of the inflation model generically reduces unless the inflatons' trajectory converge well at least on the CMB scale. In our hybrid inflation case, the CMB scale mode exits the horizon in the well-converging valley phase, and indeed the result is not affected by the initial condition so much.

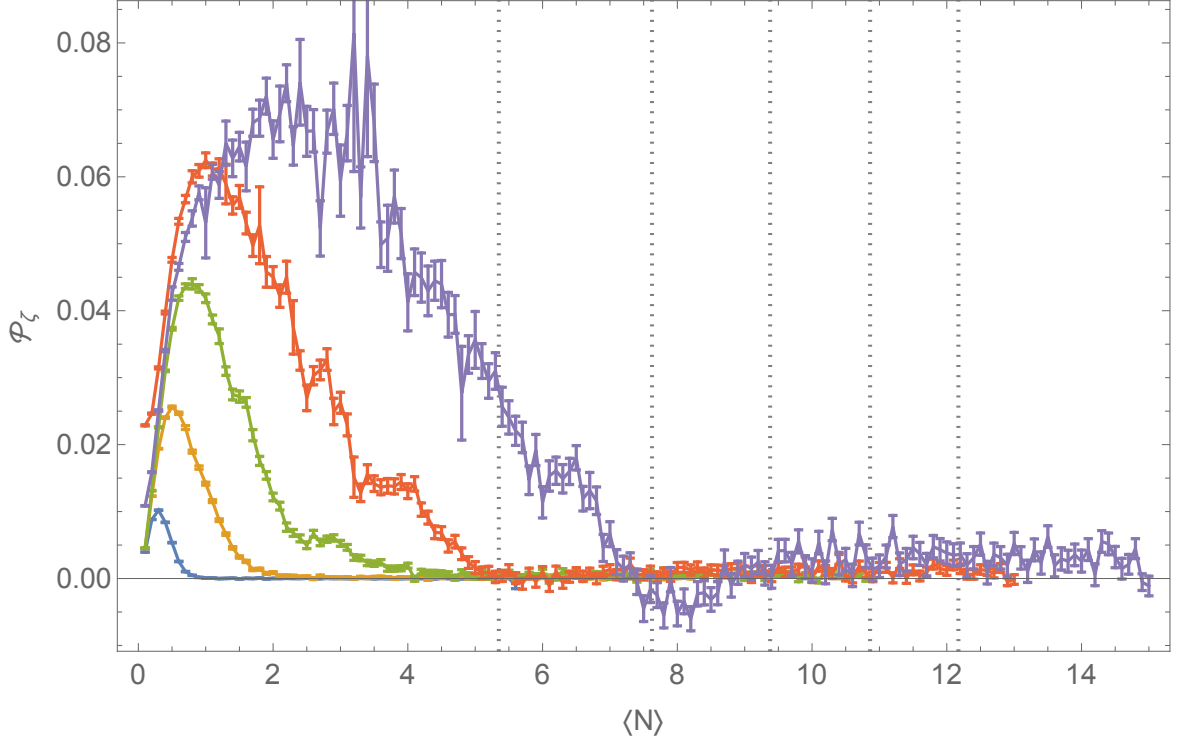


Figure 4. The power spectrum calculated in the stochastic- δN algorithm [34, 35]. Each power spectrum is averaged over 10000 sample paths and on each data point 1000 paths are made for each sample path. The error bars represent the standard errors. From bottom to top, $\Pi^2 = 10, 20, 30, 40$, and 50. Also from left to right, the vertical gray dotted lines represent the times when the paths pass the critical point for $\Pi^2 = 10$ to 50. It suggests that it takes about 10 e-folds for the curvature perturbations to grow up maximally from the critical point. Therefore the power spectrum has a peak almost around the end of inflation for low Π^2 and this validates the procedure in the previous section.

for the curvature perturbations to grow up maximally from the critical point. Therefore the power spectrum necessarily has a peak almost around the end of inflation for low Π^2 with which the waterfall phase continues less than about 10 e-folds. This result validates that we used the curvature perturbations coarse-grained on the Hubble scale at the end of inflation to obtain the PBH abundance in the previous section.

5 Conclusions

In this paper we study the possibility whether massive PBHs can be produced in mild-waterfall hybrid inflation whose potential can be parametrized as eq. (2.2). As a recent related work, Clesse and Garcia-Bellido (CG) [32] estimated the curvature perturbations during the waterfall phase in the linear δN formalism and found that the results depend almost only on the specific parameter combination $\Pi^2 = M^2 \phi_c \mu_1 / M_p^4$ as briefly reviewed in section 2. However, since the waterfall field dynamics is dominated by the Hubble fluctuations around the critical point, one must go beyond the linear perturbation theory to calculate the curvature perturbations. Accordingly we calculate the curvature perturbations without perturbative expansions with respect to the scalar fields, combining the stochastic and δN formalism.

In section 3, the variance of the curvature perturbations is calculated for various parameter values as shown in figure 1, and it shows that indeed the curvature perturbations depend almost only on Π^2 though there are factor differences between our and CG's result. Subsequently we estimate the PBH abundance with use of this variance including the non-Gaussian effect as plotted in figure 2. The abundance is calculated both for the simple assumption of the threshold, namely $\zeta_c = 1$, and the recent analytic work $\zeta_c \simeq 0.086$ [52]. As a result, the specific parameter combination $\Pi^2 = M^2 \phi_c \mu_1 / M_p^4$ should be less than around 11 not to overproduce PBHs if $\zeta_c = 1$, which means that the waterfall phase can continue only 4–5 e-folds at most. Also, if $\zeta_c \simeq 0.086$, Π^2 should be smaller than ~ 1 .

As a worth noting point, the curvature perturbations calculated in the stochastic formalism are coarse-grained on the horizon scale at the end of inflation. Therefore the obtained abundance is for the PBHs whose mass corresponds with that scale. In section 4, we calculate the power spectrum of the curvature perturbations for low Π^2 with use of the algorithm proposed in [34], and the results are shown in figure 4. It shows that indeed the power spectrum has a peak almost around the end of inflation for low Π^2 , and therefore the above procedures are verified.

In summary, the specific parameter combination $\Pi^2 = M^2 \phi_c \mu_1 / M_p^4$ should be less than around 11 for $\zeta_c = 1$ and then the waterfall phase cannot continue so long. Moreover in such cases the power spectrum shows a sharp peak near the end of inflation and therefore the PBH mass scale given by the horizon scale at the end of inflation, that is, $M_{\text{PBH}} \sim \frac{M_p^2}{H_{\text{inf}}} \simeq 10^4 \text{ g} \left(\frac{H_{\text{inf}}}{10^9 \text{ GeV}} \right)^{-1}$. It is much smaller than desired one (comparable to $M_\odot \sim 10^{33} \text{ g}$) because the corresponding scale does not benefit by the exponential inflating during the waterfall phase.

Acknowledgments

This work is supported by MEXT KAKENHI Grant Number 15H05889 (M. K.), JSPS KAKENHI Grant Number 25400248 (M. K.) and also by the World Premier International Research Center Initiative (WPI), MEXT, Japan. Y. T. is supported by a JSPS Research Fellowship for Young Scientists.

References

- [1] S. Hawking, Mon. Not. Roy. Astron. Soc. **152**, 75 (1971).
- [2] B. J. Carr and S. W. Hawking, Mon. Not. Roy. Astron. Soc. **168**, 399 (1974).
- [3] B. J. Carr, Astrophys. J. **201**, 1 (1975). doi:10.1086/153853
- [4] K. Griest, A. M. Cieplak and M. J. Lehner, Phys. Rev. Lett. **111**, no. 18, 181302 (2013).
- [5] F. Capela, M. Pshirkov and P. Tinyakov, Phys. Rev. D **87**, no. 12, 123524 (2013) [arXiv:1301.4984 [astro-ph.CO]].
- [6] P. Pani and A. Loeb, JCAP **1406**, 026 (2014) doi:10.1088/1475-7516/2014/06/026 [arXiv:1401.3025 [astro-ph.CO]].
- [7] F. Capela, M. Pshirkov and P. Tinyakov, arXiv:1402.4671 [astro-ph.CO].
- [8] G. Defillon, E. Granet, P. Tinyakov and M. H. G. Tytgat, Phys. Rev. D **90**, no. 10, 103522 (2014) doi:10.1103/PhysRevD.90.103522 [arXiv:1409.0469 [gr-qc]].

- [9] J. Kormendy and D. Richstone, *Ann. Rev. Astron. Astrophys.* **33**, 581 (1995).
doi:10.1146/annurev.aa.33.090195.003053
- [10] X. Fan *et al.* [SDSS Collaboration], *Astron. J.* **122**, 2833 (2001) doi:10.1086/324111
[astro-ph/0108063].
- [11] D. J. Mortlock *et al.*, *Nature* **474**, 616 (2011) doi:10.1038/nature10159 [arXiv:1106.6088
[astro-ph.CO]].
- [12] R. Bean and J. Magueijo, *Phys. Rev. D* **66**, 063505 (2002) [astro-ph/0204486].
- [13] M. Kawasaki, N. Sugiyama and T. Yanagida, *Phys. Rev. D* **57**, 6050 (1998) [hep-ph/9710259].
M. Kawasaki and T. Yanagida, *Phys. Rev. D* **59**, 043512 (1999) [hep-ph/9807544].
- [14] J. Yokoyama, *Phys. Rev. D* **58**, 083510 (1998) [astro-ph/9802357].
- [15] T. Kawaguchi, M. Kawasaki, T. Takayama, M. Yamaguchi and J. Yokoyama, *Mon. Not. Roy. Astron. Soc.* **388**, 1426 (2008) [arXiv:0711.3886 [astro-ph]].
- [16] P. H. Frampton, M. Kawasaki, F. Takahashi and T. T. Yanagida, *JCAP* **1004**, 023 (2010)
[arXiv:1001.2308 [hep-ph]].
- [17] K. Kohri, D. H. Lyth and A. Melchiorri, *JCAP* **0804**, 038 (2008) [arXiv:0711.5006 [hep-ph]].
- [18] M. Drees and E. Erfani, *JCAP* **1104**, 005 (2011) [arXiv:1102.2340 [hep-ph]].
M. Drees and E. Erfani, *JCAP* **1201**, 035 (2012) [arXiv:1110.6052 [astro-ph.CO]].
- [19] M. Kawasaki, N. Kitajima and T. T. Yanagida, *Phys. Rev. D* **87**, no. 6, 063519 (2013)
[arXiv:1207.2550 [hep-ph]].
- [20] A. D. Linde, *Phys. Rev. D* **49**, 748 (1994) [astro-ph/9307002].
- [21] G. R. Dvali, Q. Shafi and R. K. Schaefer, *Phys. Rev. Lett.* **73**, 1886 (1994) [hep-ph/9406319].
- [22] W. Buchmuller, L. Covi and D. Delepine, *Phys. Lett. B* **491**, 183 (2000) [hep-ph/0006168].
W. Buchmuller, V. Domcke and K. Schmitz, *Nucl. Phys. B* **862**, 587 (2012) [arXiv:1202.6679
[hep-ph]].
W. Buchmuller, V. Domcke, K. Kamada and K. Schmitz, *JCAP* **1407**, 054 (2014)
[arXiv:1404.1832 [hep-ph]].
- [23] P. A. R. Ade *et al.* [Planck Collaboration], arXiv:1502.01589 [astro-ph.CO].
P. A. R. Ade *et al.* [Planck Collaboration], arXiv:1502.02114 [astro-ph.CO].
- [24] S. Clesse, *Phys. Rev. D* **83**, 063518 (2011) [arXiv:1006.4522 [gr-qc]].
- [25] H. Kodama, K. Kohri and K. Nakayama, *Prog. Theor. Phys.* **126**, 331 (2011)
doi:10.1143/PTP.126.331 [arXiv:1102.5612 [astro-ph.CO]].
- [26] D. Mulryne, S. Orani and A. Rajantie, *Phys. Rev. D* **84**, 123527 (2011)
doi:10.1103/PhysRevD.84.123527 [arXiv:1107.4739 [hep-th]].
- [27] S. Clesse and B. Garbrecht, *Phys. Rev. D* **86**, 023525 (2012) doi:10.1103/PhysRevD.86.023525
[arXiv:1204.3540 [hep-ph]].
- [28] S. Clesse, B. Garbrecht and Y. Zhu, *Phys. Rev. D* **89**, no. 6, 063519 (2014)
doi:10.1103/PhysRevD.89.063519 [arXiv:1304.7042 [astro-ph.CO]].
- [29] J. Garcia-Bellido, A. D. Linde and D. Wands, *Phys. Rev. D* **54**, 6040 (1996) [astro-ph/9605094].
- [30] D. H. Lyth, *JCAP* **1107**, 035 (2011) [arXiv:1012.4617 [astro-ph.CO]].
D. H. Lyth, *JCAP* **1205**, 022 (2012) [arXiv:1201.4312 [astro-ph.CO]].
- [31] E. Bugaev and P. Klimai, *JCAP* **1111**, 028 (2011) [arXiv:1107.3754 [astro-ph.CO]].
E. Bugaev and P. Klimai, *Phys. Rev. D* **85**, 103504 (2012) [arXiv:1112.5601 [astro-ph.CO]].
- [32] S. Clesse and J. Garcia-Bellido, *Phys. Rev. D* **92**, no. 2, 023524 (2015) [arXiv:1501.07565
[astro-ph.CO]].

- [33] J. Martin and V. Vennin, *Phys. Rev. D* **85**, 043525 (2012) doi:10.1103/PhysRevD.85.043525 [arXiv:1110.2070 [astro-ph.CO]].
- [34] T. Fujita, M. Kawasaki, Y. Tada and T. Takesako, *JCAP* **1312**, 036 (2013) [arXiv:1308.4754 [astro-ph.CO]].
- [35] T. Fujita, M. Kawasaki and Y. Tada, *JCAP* **1410**, no. 10, 030 (2014) [arXiv:1405.2187 [astro-ph.CO]].
- [36] V. Vennin and A. A. Starobinsky, *Eur. Phys. J. C* **75**, 413 (2015) doi:10.1140/epjc/s10052-015-3643-y [arXiv:1506.04732 [hep-th]].
- [37] A. A. Starobinsky, *Lect. Notes Phys.* **246**, 107 (1986). doi:10.1007/3-540-16452-9_6
- [38] Y. Nambu and M. Sasaki, *Phys. Lett. B* **205**, 441 (1988). doi:10.1016/0370-2693(88)90974-4
Y. Nambu and M. Sasaki, *Phys. Lett. B* **219**, 240 (1989). doi:10.1016/0370-2693(89)90385-7
- [39] H. E. Kandrup, *Phys. Rev. D* **39**, 2245 (1989). doi:10.1103/PhysRevD.39.2245
- [40] K. i. Nakao, Y. Nambu and M. Sasaki, *Prog. Theor. Phys.* **80**, 1041 (1988). doi:10.1143/PTP.80.1041
Y. Nambu, *Prog. Theor. Phys.* **81**, 1037 (1989). doi:10.1143/PTP.81.1037
- [41] S. Mollerach, S. Matarrese, A. Ortolan and F. Lucchin, *Phys. Rev. D* **44**, 1670 (1991). doi:10.1103/PhysRevD.44.1670
- [42] A. D. Linde, D. A. Linde and A. Mezhlumian, *Phys. Rev. D* **49**, 1783 (1994) doi:10.1103/PhysRevD.49.1783 [gr-qc/9306035].
- [43] A. A. Starobinsky and J. Yokoyama, *Phys. Rev. D* **50**, 6357 (1994) doi:10.1103/PhysRevD.50.6357 [astro-ph/9407016].
- [44] A. A. Starobinsky, *JETP Lett.* **42**, 152 (1985) [*Pisma Zh. Eksp. Teor. Fiz.* **42**, 124 (1985)].
- [45] D. S. Salopek and J. R. Bond, *Phys. Rev. D* **42**, 3936 (1990). doi:10.1103/PhysRevD.42.3936
- [46] M. Sasaki and E. D. Stewart, *Prog. Theor. Phys.* **95**, 71 (1996) doi:10.1143/PTP.95.71 [astro-ph/9507001].
- [47] M. Sasaki and T. Tanaka, *Prog. Theor. Phys.* **99**, 763 (1998) doi:10.1143/PTP.99.763 [gr-qc/9801017].
- [48] D. H. Lyth, K. A. Malik and M. Sasaki, *JCAP* **0505**, 004 (2005) doi:10.1088/1475-7516/2005/05/004 [astro-ph/0411220].
- [49] M. Morikawa, *Phys. Rev. D* **42**, 1027 (1990). doi:10.1103/PhysRevD.42.1027
- [50] W. H. Press and P. Schechter, *Astrophys. J.* **187**, 425 (1974). doi:10.1086/152650
- [51] S. Young, C. T. Byrnes and M. Sasaki, *JCAP* **1407**, 045 (2014) [arXiv:1405.7023 [gr-qc]].
- [52] T. Harada, C. M. Yoo and K. Kohri, *Phys. Rev. D* **88**, no. 8, 084051 (2013) [*Phys. Rev. D* **89**, no. 2, 029903 (2014)] [arXiv:1309.4201 [astro-ph.CO]].
- [53] B. J. Carr, K. Kohri, Y. Sendouda and J. Yokoyama, *Phys. Rev. D* **81**, 104019 (2010) [arXiv:0912.5297 [astro-ph.CO]].
- [54] D. Jeong, “Cosmology with high ($z_i > 1$) redshift galaxy surveys,” Diss. University of Texas, 2010.